OPEN ACCESS

ORIGINAL ARTICLE

SLC39A5 mutations interfering with the BMP/TGF-β pathway in non-syndromic high myopia

Hui Guo,[1,2] Xuemin Jin,[3] Tengfei Zhu,[1] Tianyun Wang,[1] Ping Tong,[4] Lei Tian,[3] Yu Peng,[1] Liangdan Sun,[5] Anran Wan,[1] Jingjing Chen,[1] Yanling Liu,[1] Ying Li,[1] Qi Tian,[1] Lu Xia,[1] Lusi Zhang,[1] Yongcheng Pan,[1] Lina Lu,[1] Qiong Liu,[1] Lu Shen,[1] Yunping Li,[1,4] Wei Xiong,[4] Jiada Li,[1,2] Beisha Tang,[6] Yong Feng,[6] Xuejun Zhang,[5] Zhuohua Zhang,[1] Qian Pan,[1] Zhengmao Hu,[1,2] Kun Xia[1,2,7]

▶ Additional material is published online only. To view please visit the journal online (http://dx.doi.org/10.1136/jmedgenet-2014-102351).

For numbered affiliations see end of article.

Correspondence to
Professor Kun Xia and Zhengmao Hu, The State Key Laboratory of Medical Genetics, Central South University, 110 Xiangya Road, Changsha, Hunan 410078, China; xiakun@sklmg.edu.cn and huzhengmao@sklmg.edu.cn

HG, XJ and TZ contributed equally.

Received 16 February 2014
Revised 24 April 2014
Accepted 13 May 2014
Published Online First
2 June 2014

To cite: Guo H, Jin X, Zhu T, *et al*. *J Med Genet* 2014;**51**:518–525.

ABSTRACT

Background High myopia, with the characteristic feature of refractive error, is one of the leading causes of blindness worldwide. It has a high heritability, but only a few causative genes have been identified and the pathogenesis is still unclear.

Methods We used whole genome linkage and exome sequencing to identify the causative mutation in a non-syndromic high myopia family. Direct Sanger sequencing was used to screen the candidate gene in additional sporadic cases or probands. Immunofluorescence was used to evaluate the expression pattern of the candidate gene in the whole process of eye development. Real-time quantitative PCR and immunoblot was used to investigate the functional consequence of the disease-associated mutations.

Results We identified a nonsense mutation (c.141C>G: p.Y47*) in *SLC39A5* co-segregating with the phenotype in a non-syndromic severe high myopia family. The same nonsense mutation (c.141C>G:p.Y47*) was detected in a sporadic case and a missense mutation (c.911T>C:p.M304T) was identified and co-segregated in another family by screening additional cases. Both disease-associated mutations were not found in 1276 control individuals. *SLC39A5* was abundantly expressed in the sclera and retina across different stages of eye development. Furthermore, we found that wild-type, but not disease-associated SLC39A5 inhibited the expression of Smad1, a key phosphate protein in the downstream of the BMP/TGF-β (bone morphogenic protein/transforming growth factor-β) pathway.

Conclusions Our study reveals that loss-of-function mutations of *SLC39A5* are associated with the autosome dominant non-syndromic high myopia, and interference with the BMP/TGF-β pathway may be one of the molecular mechanisms for high myopia.

INTRODUCTION

Myopia, which is characterised by refractive error resulting primarily from excess elongation of the eye, is one of the most common eye disorders. The prevalence varies across countries, but is really high (~71–96%) in Asian countries such as China, Singapore, and Japan.[1–3] High myopia—clinically defined as a spherical equivalent refractive error ≥6 dioptre—affects 1–10% of the general population.[4] It may result in several severe complications including macular degeneration, retinal detachment, cataract and glaucoma, and greatly increases the risk of blindness. There are several syndromic forms of high myopia, with additional findings involving skeleton, heart, and ears such as Marfan, Stickler and the recently defined deafness and myopia syndrome.

Both environmental (close working habits, higher education levels, higher socioeconomic class, etc) and genetic factors are involved in the aetiology of myopia.[5 6] Twin and family studies demonstrated that myopia, especially high myopia, has a very high heritability.[7 8] Candidate and whole genome linkage analysis has identified dozens of loci for non-syndromic myopia, but no associated gene has been found in these linkage intervals up to now. Several genome-wide association studies (GWAS) and meta-analyses have found that myopia or refractive error is associated with common variants at *GJD2*, *RASGRF1*, *GRIA4*, *KCNQ5*, *RDH*, *LAMA2*, *BMP25*, *SIX6*, and *PRSS56*, which may involve eye development by regulating ion transport, neurotransmission, retinoic acid metabolism, and extracellular matrix remodelling.[9–12] Several other susceptible genes or loci were also identified, increasing the risk of high myopia by GWAS, such as *CTNND2*, 1q41, *ZC3H11B*, *SNTB1*, *VIPR2*, and *ZFHX1B*.[13–17] Recently, by using family based conversional positional cloning or exome sequencing, four genes (*ZNF644*,[18] *SCO2*,[19] *LEPREL1*,[20] *LRPAR1*[21]) have been identified in monogenic non-syndromic high myopia families. However, all these genes can only explain a very small proportion of high myopia subjects and the pathogenesis is still unclear.

In this study, we recruited a three-generations Chinese high myopia family with autosomal dominant inheritance. By using whole genome linkage and exome sequencing, we identified a segregating nonsense mutation of *SLC39A5* in this family. Candidate screening in other high myopia families and sporadic samples identified another family with a missense mutation and a sporadic case with the same nonsense mutation. Immunofluorescence revealed that SLC39A5 involves the whole process of eye development and expresses mainly in sclera and retina. Real-time quantitative PCR (qPCR) and immunoblot showed that both disease-associated

mutations are loss-of-function and interfere with the BMP/TGF-β (bone morphogenic protein/transforming growth factor-β) pathway.

METHODS

Study subjects and clinical characterisation

A Chinese Henan non-syndromic high myopia family (HM-FR3) with autosomal dominant inheritance participated in this study (figure 1A). All recruited members underwent clinical examination and blood collection after providing informed consent. All of the affected cases have a history of myopia onset before 10 years of age. A comprehensive ophthalmic examination was performed and the refractive error and axial length were measured and recorded. All of the affected individuals have no known ocular disease or insult that could predispose to myopia, such as retinopathy of prematurity or early age media opacification, and no known genetic diseases associated with myopia, such as Stickler or Marfan syndrome. The study was approved by the Institutional Review Board of The State Key Laboratory of Medical Genetics and adhered to the tenets of the Declaration of Helsinki.

Whole genome genotyping and linkage analysis

Genomic DNA was extracted from leucocytes of all individuals by the standard proteinase K digestion and phenol-chloroform method. Whole genome genotyping was performed using Illumina HumanLinkage-12 Bead Chip on all recruited members of pedigree HM-FR3, strictly following the instructions of Illumina's protocol. Genotype calling and quality control were performed using the Illumina GenomeStudio Genotyping Module (V6.0). Single nucleotide polymorphisms (SNPs) were excluded if the call rate was lower than 95%, departed from Hardy-Weinberg equilibrium ($p<0.001$) or had Mendelian inconsistencies. Finally, the call rates for all individuals were above 98% and a total of 5440 autosomal SNPs were left for linkage analyses. Parametric two-point and multi-point linkage analysis using the genotypes after quality control were carried out with MERLIN[22] based on an autosomal

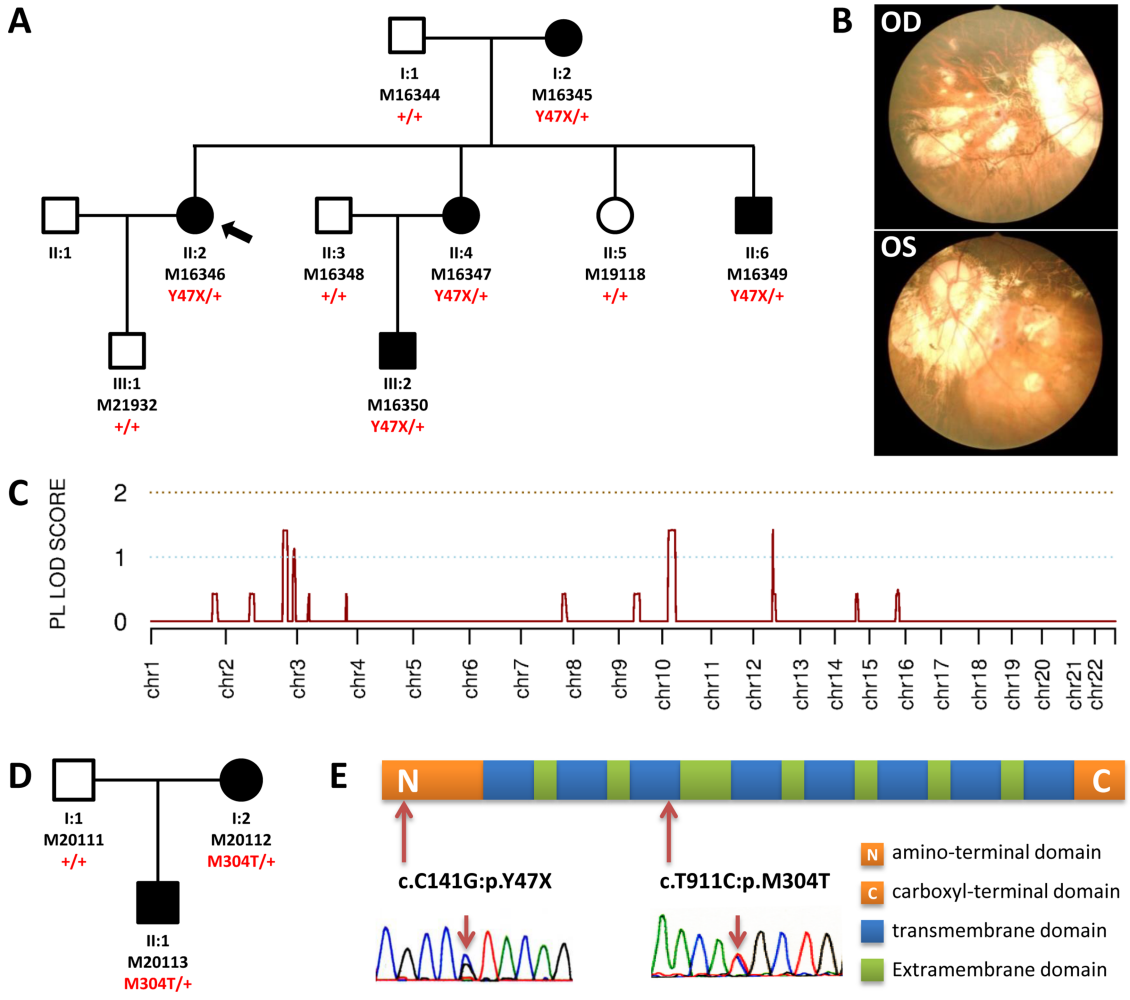

Figure 1 Identification of *SLC39A5* mutations in high myopia patients. (A) The pedigree plot for HM-FR3: solid symbols represent affected individuals. M numbers denote individuals whose DNA samples were analysed. The nonsense mutation (Y47X) identified by whole genome linkage and exome sequencing segregated with the phenotype exactly. (B) Fundus photograph for the proband of HM-FR3 (M16346) appeared tigroid and had focal atrophy of the choroid. OD represents right eye and OS represents left eye. (C) Multi-point parametric linkage analysis shows four regions with LOD score more than 1 on chromosome 2, 10, and 12, respectively, and other eight low peaks with maximum LOD score no more than 0.5. (D) The pedigree plot for family HM-ZZ19 with the missense mutation (M304T) of *SLC39A5*. (E) Schematic of human SLC39A5 protein structure and mutational locations: the nonsense mutation occurred at the 47th amino acid and is located in the amino-terminal domain; the missense mutation is located at the terminal of the third transmembrane domain.

dominant (AD) model with 0.9 penetrance and an allele frequency of 0.01. The affection statuses were defined strictly according to the clinical diagnosis.

Targeted region capturing and exome sequencing

For each patient selected for exome sequencing, 1 μm of genomic DNA was fragmented and selected, aiming for a 350–400 base pair product and PCR amplified. Exome capturing was performed to collect the protein coding regions of human genome DNA using Illumina TruSeq array as described in the manufacturer's instructions. The exon-enriched DNA libraries were sequenced using the Illumina HiSeq 2000 platform, following the manufacturer's instructions (Illumina, San Diego, USA).

Read mapping, variant analysis, and mutation validation

Generated reads by exome sequencing were aligned to human reference genome hg19 (UCSC version) using BWA (Burrows-Wheeler Aligner) 0.5.6.[23] Read qualities were recalibrated using GATK Table Recalibration 1.0.2905.[24] Picard 1.14 was used to flag duplicate reads (http://picard.sourceforge.net/). GATK IndelRealigner 1.0.2905 was used to realign reads around insertion/deletion (InDel) sites. Single nucleotide variants (SNVs) were generated with GATK Unified Genotyper[24] and in parallel with the SAM tools pipeline.[25] The small InDels were also called with the GATK Unified Genotyper and SAMtools. The called SNVs and InDels are annotated with ANNOVAR,[26] and filtered as follows: (1) extracting non-synonymous, splicing, and InDel variants; (2) excluding high frequency (minor allele frequency (MAF) >0.01) polymorphisms in dbSNP137, 1000 genome and ESP6500; (3) extracting heterozygous variants; (4) excluding variants in our 50 in-house control samples with exomeSeq data; (5) extracting the shared variants of the two affected individuals; (6) extracting the variants located in the linkage signal regions. Sanger sequencing was used to validate the co-segregating status of the mutations left by the above filtering procedures. Mutation screening in the 180 probands and sporadic cases was also performed by Sanger sequencing. The primer pairs spanning all exons, untranslated regions (UTRs) and splicing sites were designed by the Primer3 program (http://frodo.wi.mit.edu/).

Immunofluorescence for expression distribution of Slc39a5 in the mouse eyes

The whole mouse embryos at embryonic day 10 and at postnatal days 0, 13, and 50 were cryopreserved according to standard procedures. The cryosections (10 μm) were incubated with haematoxylin and eosin, anti-Slc39a5 (Sigma-Aldrich), or a rabbit IgG isotype negative control (Vector labs). Bound primary antibody was detected with Alexa Fluor 488-conjugated secondary antibody (Jackson), and the nuclei were counter-stained with DAPI (4',6-diamidino-2-phenylindole) (Invitrogen). Immunofluorescence was analysed with an Eclipse TE2000-E inverted confocal microscope (Leica Instruments).

Real-time qPCR

Total RNA was isolated from lymphocyte cell lines from the patients and unaffected family members using the GeneJET RNA purification kit (Fermentas), as described by the manufacturer. First strand cDNA was synthesised with Revert Aid First Strand cDNA Synthesis Kit (Fermentas) from total RNA. Quantitative PCR was performed with the Maxima SYBR Green qPCR Master Mix (Fermentas) for SLC39A5 mRNA (forward primer, 5′-CTCGTCAGTTTGCTCTGCTG; reverse primer, CAGCAAGGGCCGTAGTAGAC) or Smad1 mRNA (forward primer, 5′-GCCCTGTACTTCCTCCTGTG; reverse primer, 5′-TTGGGTTGCTGGAAAGAATC). ACTB (forward primer, 5′-AATCTGGCACCACACCTTCTA; reverse primer, 5′-GAT AGCAACGTACATGGCTGG) and 18S rRNA (forward primer, 5′-AGTCCCTGCCCTTTGTACACA; reverse primer, CGATCCGAGGGCCTCACTA) were used for normalisation in mRNA relative quantifications. All samples were run in triplicate. Relative SLC39A5 mRNA levels or Smad1 mRNA levels were normalised to that of ACTB or 18S rRNA, calculated by the $2^{-\Delta\Delta Ct}$ method and log10 transformed. A value of $p<0.05$ was considered to be statistically significant.

Immunoblot analyses

Cells were seeded in 24-well plates transfected with empty SLC39A5-FLAG, SLC39A5-M304T-FLAG or SLC39A5-Y46X-FLAG plasmid using Lipofectamine 2000 (Invitrogen). Cells were harvested 48 h after transfection for protein extraction. Cells were lysed and homogenised with SDS (sodium dodecyl sulfate) sample buffer (63 mM Tris-HCl, 10% glycerol, 2% SDS) and Protease Inhibitor Cocktail (Sigma). Twenty micrograms of total protein per lane were separated on 10% SDS-PAGE (polyacrylamide gel electrophoresis) gels and followed by transfer to PVDF membranes (Millipore). Membranes were blocked by 5% non-fat milk for 1 h at room temperature followed by incubation overnight with primary antibody at 4. The antibody used was rabbit-anti Smad1 (Cell Signaling), M2 (Sigma), mouse-anti SLC39A5 (sigma), mouse-anti β-actin (Sigma).

SLC39A5 shRNA plasmid construction

The short hairpin RNA targeting SLC39A5 cDNA was designed with Block-iT RNAi Designer (Invitrogen). SLC39A5 sh1 (5′-GGAATCTCGAAACACGCAACT-3′), SLC39A5 sh2 (5′-GACCACCTGAATGAGGATTGT-3′), SLC39A5 sh3 (5′-GCCCTGCTTTATCAGATCGAC-3′), and a control shRNA (5′-GACTCACGCATCGAACAATGA-3′), which was not homologous with any known mammal genes, were used in the experiment. Oligonucleotides were annealed followed by insertion into pSUPER vector (OligoEngine).

Immunofluorescence for subcellular localisation of SLC39A5

Cells were cultured on glass coverslips. Wide type and mutant vectors were transfected by lipo2000 (Invitrogen). The cells were then fixed in 4% paraformaldehyde/sucrose for 10 min. Cell permeabilisation was performed with 0.1% Triton X-100/PBS (phosphate buffered saline) for 15 min followed by blocking with BSA (bovine serum albumin) for 30 min. The cells were then probed by primary antibody and stained by Alex Flour 488-conjugated or cy3-conjugated second antibody. DAPI was used for nuclear stain. Images were acquired with an Eclipse TCS-SP5 inverted confocal microscope (Leica).

RESULTS

Clinical description

Nine members (five affected, figure 1A) of HM-FR3 were recruited into the study. The refractive errors for the five affected subjects range from −5.00 to −25.00 dioptre sphere (DS) for the left eye (OS) and from −7.00 to −20.00 DS for the right eye (OD). Eye globe axial length ranges from 26.14 to 33.32 mm for OS and 26.29 to 32.09 mm for OD (table 1). The proband (M16346) and two elderly patients showed typical fundus features of high myopia, tigroid and focal atrophy of choroid (figure 1B). All of the affected individuals have a history of myopia onset before the age of 10 years old (table 1)

Table 1 Description of clinical characteristics of the family members and the sporadic case with *SLC39A5* mutations

Sample ID	Sex	Affection status	Age at onset (years)	Age at exam (years)	Corneal power		Refractive error (DS)		Axial length (mm)		Mutations
					OD	OS	OD	OS	OD	OS	
HM-FR3											
M16344	M	U	NA	70	42.75/43.01	42.50/44.62	−0.34	−0.50	24.2	23.8	NO
M16345	F	A	10	68	43.50/44.75	43.01/44.25	−5.00	−7.00	26.14	27.65	c.C141G:p.Y47X
M16346	F	A	3	47	41.57/42.75	42.01/43.50	−25.00	−20.00	33.32	32.09	c.C141G:p.Y47X
M16348	M	U	NA	44	40.65/41.34	40.50/42.45	+1.00	+0.50	23.5	23.9	NO
M16347	F	A	5	42	41.75/42.23	41.50/42.35	−9.00	−13.00	28.13	29.41	c.C141G:p.Y47X
M19118	F	U	NA	28	41.21/43.89	41.50/43.25	−0.30	−0.25	24.0	24.5	NO
M16349	M	A	8	35	42.35/44.62	42.75/44.25	−5.00	−7.00	27.87	28.52	c.C141G:p.Y47X
M16350	M	A	8	15	43.25/44.00	43.75/44.50	−7.50	−7.00	26.35	26.29	c.C141G:p.Y47X
M21932	M	U	NA	17	42.75/43.50	42.02/43.65	−0.22	−0.45	23.8	24.1	NO
HM-ZZ19											
M20111	M	U	NA	50	40.87/41.50	40.25/42.50	−1.00	−1.00	23.9	24.00	NO
M20112	F	A	10	48	43.19/44.25	43.94/45.25	−8.00	−8.50	27.50	28.35	c.T911C:p.M304T
M20113	M	A	5	23	43.75/44.12	44.00/45.25	−6.50	−5.25	26.54	26.52	c.T911C:p.M304T
Sporadic											
M21789	M	A	9	45	41.26/42.79	41.38/43.21	−20.00	−18.50	31.34	29.58	c.C141G:p.Y47X

OD represents right eye and OS represents left eye.
A, affected; DS, diopter sphere; F, female; M, male; U, unaffected.

and have no known ocular disease or insult that could predispose to myopia.

Whole genome linkage and exome sequencing identified segregating mutation in SLC39A5

To narrow the chromosome intervals and increase the possibility of identifying the causative mutation, we firstly performed whole genome linkage analysis using Illumina Human Linkage-12 BeadChip. Multi-point parametric linkage analysis identified four regions on chromosome 2, 10, and 12 with maximum multi-point parametric LOD (logarithm of odds) scores from 1 to 1.42 (figure 1C, see online supplementary table S1). We also identified eight other signals distributed in seven chromosomes, with maximum parametric and non-parametric LOD scores of no more than 0.5 (figure 1C). Nevertheless, we also included these eight signals in the following filtering procedures as linkage intervals.

We subsequently performed exome capturing and sequencing for two patients (M16346 and M16350, figure 1A) from family HM-FR3. In total, we generated an average of 6.38 Gbp and 13.09 Gbp of sequence with more than 50× and 90× coverage for each individual as paired-end, 110-bp reads, and more than 95% of the targeted bases were covered sufficiently to pass our thresholds for calling SNVs and insertions and deletions (InDels) (see online supplementary table S2). We identified 21 963 (9083 non-synonymous SNV, splicing SNV and InDels) and 21 047 (8679 non-synonymous SNV, splicing SNV and InDels) coding variants in M16346 and M16350, respectively. The called SNVs and InDels were filtered as described in the method (Read mapping, variant analysis and mutation validation). Following the filtering procedures described above, only four variants were left for our further analysis (table 2). We used Sanger sequencing to validate these four variants and analyse the co-segregating status of the variants in all family members. Finally, only one nonsense mutation in *SLC39A5* (c.141C>G:p.Y47*) co-segregated with the phenotype in all family members. Considering that the HM-FR3 family is not large enough to detect complete linkage signals (the MAX-LOD score is 1.42), we also assessed all the variants shared between the two affected individuals (left by procedure 5). Only the nonsense mutation in *SLC39A5* co-segregated with the phenotype in all family members.

This mutation is located in the linkage region in chromosome 12 with the maximum multi-point parametric LOD score of 1.42 (rs774033 and rs10122, see online supplementary table S1). To confirm that the segregating status of the mutation is consistent with the haplotype segregating status, we performed the haplotype analysis using the genotyped SNPs around this mutation. The haplotype plot shows that the mutation segregated within the haplotype exactly (see online supplementary figure S1). This mutation is not identified in 500 population-matched controls using Sanger sequencing, or

Table 2 Filtering procedures and statistics for the SNVs and InDels called from the exome sequencing data

Sample ID	NS/SS/InDel	LowFreq (MAF<0.01)	Dominant (Heterozygous)	Absent in our 50 exomeSeq data	Segregating in exomeSeq subjects	In linkage regions	Segregating in all family members
M16346	8692/77/313	630/26/291	622/21/202	437/8/46	72/2/6	3/1/0	1/0/0 (*SLC39A5*:c.C141G:p.Y47X)
M16350	8300/69/309	549/19/293	540/14/195	385/3/39			

InDel, insertions and deletions; LowFreq represents low allele frequency (MAF<0.01) both in 1000g2012Aril and ESP6500NS, non-synonymous variants; SNV, single nucleotide variant; SS, splicing variants.

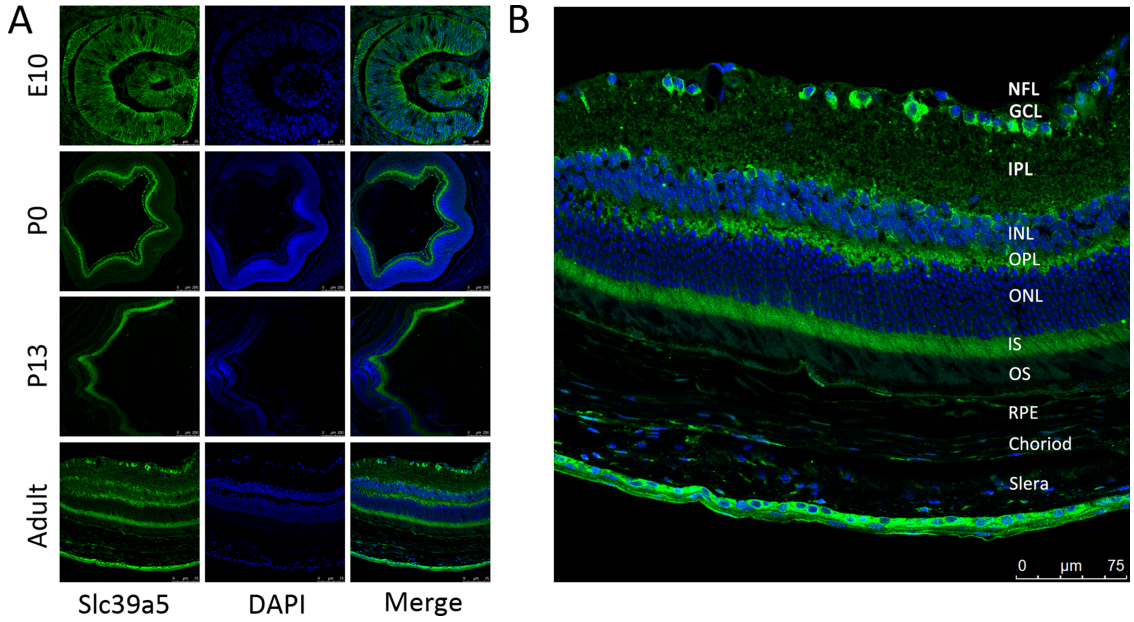

Figure 2 Slc39a5 is expressed in all stages of developing mouse eye, mainly in the sclera and retina. (A) Immunofluorescent labelling of Slc39a5 at different developing stages of normal mouse eye. The localisation of Slc39a5 is shown by the green colour, and the blue colour indicates the nuclei that were stained with DAPI. We selected four developing stages of normal mouse, E10, P0, P13, and adult. Slc39a5 is abundantly expressed at different developing stages of the eye. (B) The enlargement of the retina and sclera from labelled adult mouse eye. Slc39a5 is abundantly expressed at the sclera and different layers of the retina. The following abbreviations represent the retinal layers: NFL, nerve fibre layer; GCL, ganglion cell layer; IPL, inner plexiform layer; INL, inner nuclear layer; OPL, outer plexiform layer; ONL, outer nuclear layer; IS, inner segment; OS, outer segment ; PRL, photo receptor layer; and RPE, retinal pigment epithelium.

in another cohort of 776 population-matched controls with exome sequencing data. High myopia and other related syndromes were excluded for all of the 1276 controls.

To validate the association of *SLC39A5* with HM, we sequenced all the exons and splice sites of this gene in a cohort of 180 patients with high myopia (63 family probands and 117 sporadic cases). The 180 patients had refractive errors ranging from −6.4 to −30.0 DS and an axial eye globe length from 26.00 to 44.38 mm for both eyes (see online supplementary table S3). Two mutations were identified. One of them (c.141C>G:p.Y47*), identified in a sporadic case (M21789, table 1), is the same as that we identified in pedigree HM-FR3. The other one (c.911T>C:p.M304T) was identified and co-segregated in a pedigree with three members (HM-ZZ19, figure 1D, table 1). The c.911T>C mutation was not identified in 1276 population-matched controls.

SLC39A5 is expressed in the sclera and retina across different stages of eye development

SLC39A5 encodes solute carrier family 39, member 5 (SLC39A5 or ZIP5), a member of the ZIP family of transporters for metal ion, specific for zinc.[27] It is reported that SLC39A5 is situated in the Golgi membrane[27] or cell membrane.[28] However, our data showed that it is localised in the membrane of endoplasmic reticulum in HEK293 cells (see online supplementary figure S2–3). Although *SLC39A5* has been shown to express in several tissues important for zinc homeostasis, including the intestine, pancreas, liver and kidney,[27] no data revealed its expression in ocular tissues. In light of further association between *SLC39A5* and high myopia and the substructure localisation of SLC39A5 in the eye, we investigated the expression of Slc39a5 in the mouse eyes with a rabbit polyclonal antiserum against Slc39a5. As shown in figure 2A, B, Slc39a5 was observed in all stages of eye development and mainly expressed in the sclera and several layers of the retina, such as the inner segment (IS), outer plexiform layer (OPL), and ganglion cell layer (GCL).

Disease-associated mutations are loss-of-function and interfere with the BMP/TGF-β pathway

Human SLC39A5 contains eight transmembrane domains, and the N-terminus and C-terminus are extra-cytosolic. There are four potential sites of N-glycosylation: three of them (Asn-49, Asn-91, and Asn-158) are found in the amino-terminal domain, and the other one (Asn-390) is predicted to lie within transmembrane domain 4. The Y47* mutation introduced a stop codon at position 47 (figure 1E). The protein level in the patients' lymphocyte cell lines was decreased compared to the normal controls as demonstrated by immunoblot, but the mRNA expression level was not different between cases and controls (see online supplementary figure S4). This indicates that the Y47* mutation may produce a truncated protein with 46 amino acids. The missense mutation was located in the third transmembrane domain (figure 1E); however, it did not influence the localisation of SLC39A5 in the membrane of endoplasmic reticulum (see online supplementary figure S3).

SLC39A13, a homologue of *SLC39A5*, encoding another zinc transporter, has been identified as causing Ehlers-Danlos syndrome (EDS).[29] EDS patients also presented with incomplete penetrance of myopia and under-hydroxylated lysyl and prolyl residues of collagens. Interestingly, Slc39a13-deficient mouse showed a disrupted BMP/TGF-β transduction pathway.[30] To see if *SLC39A5* is also involved in the BMP/TGF-β pathway, the expression of Smad1, a key downstream transcription factor, was examined by real-time qPCR and immunoblot. As shown in figure 3A, B, we observed pronounced upregulation of Smad1 in both mRNA (figure 3A, see online supplementary figure S5)

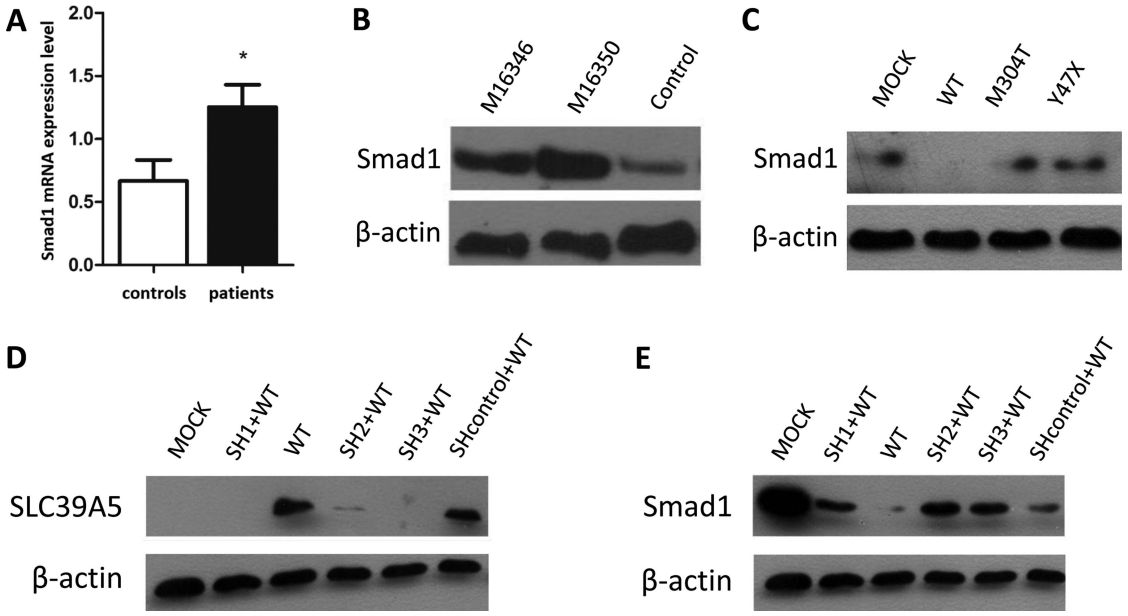

Figure 3 Disease-associated mutations of *SLC39A5* failed to suppress Smad1 expression. (A, B) Real-time quantitative PCR and immunoblot analysis showed a pronounced increase of both mRNA (A) and protein (B) expression level of Smad1 in two affected individuals (M16346 and M16350) as compared to controls. (C) Immunoblot analysis showed that wild-type SLC39A5 suppressed Smad1 expression; however, both disease-associated mutations notably up-regulated Smad1expression in transduced HEK293 cell lines. (D, E). Immunoblot analysis showed that SLC39A5 shRNAs (SH1, SH2, SH3) (D) notably attenuated the suppressive effect of wild-type SLC39A5 on Smad1 expression (E).

and protein (figure 3B) expression levels in the patients' lymphocyte cell lines as compared to controls. We also demonstrated that wild type, but not disease-associated SLC39A5, suppressed the expression of Smad1 in HEK293 cells (figure 3C). To further study the effect of SLC39A5 on the Smad1 expression, we transduced HEK293 cells with three SLC39A5 shRNA vector (SH1, SH2, SH3). As shown in figure 3D,E, silence of SLC39A5 significantly attenuated the suppressive effect of wild-type SLC39A5 on Smad1 expression, implying the disease-associated mutations are loss-of-function. As the BMP/TGF-β pathway has been recurrently implicated in myopia development,[21 31 32] disruption of the BMP/TGF-β pathway may be one of the mechanisms underlying high myopia.

DISCUSSION

We have identified that loss-of-function mutations in *SLC39A5* were associated with high myopia by using the combination of whole genome linkage analysis and exome sequencing. Our data indicate that Slc39a5 was highly expressed in all developing stages of mouse eyes and mainly expressed in sclera and retina, further implying the association between *SLC39A5* and eye development. Functional studies indicated that wild-type, but not disease-associated SLC39A5 suppressed the expression of Smad1, suggesting disruption in the BMP/TGF-β pathway as one of the underlying mechanisms of high myopia.

The disease-associated nonsense mutation Y47* has been annotated as an extremely rare SNP (rs199624584). One individual (HG00701) from the Chinese population in the 1000 genome project carried this variant. Since there is no phenotype record in the 1000 genome samples, it is unclear whether the individual has the myopia phenotype or not. The missense variant is a private mutation which has not been reported in any database and our 1276 controls. It is located in the fourth transmembrane domain. The functional prediction of this mutation by SIFT and PolyPhen2 is not damaging. However, our functional analysis demonstrated that it has a pathogenic effect. We revealed that this variant, as with Y47*, lost the function to suppress Smad1 expression. SLC39A5 has been reported suiting in Golgi[27] or plasma membrane.[28] However, we revealed that SLC39A5 is localised in the membrane of the endoplasmic reticulum in HEK293 cells. The most likely explanation is that different cell types were used in these studies. It is reported that one protein can localise in different subcellular structures to play different functions in different cells. This phenomenon has been observed in other genes, such as *TLR3*[33] and *GPR30*.[34]

SLC39A5 encodes a zinc transporter. Interestingly, zinc is essential for eye development and zinc deficiency has been reported in high myopia patients.[35 36] Our data show that zinc transporter Slc39a5 is involved in the whole stage of mouse eye development and is abundantly expressed in the sclera and retina. Although it is still unclear how zinc participates in eye development and the development of myopia, we identified that disease-associated mutations of the zinc transporter encoded the gene dysregulated BMP/TGF-β pathway. Interestingly, TGF-β is one of the most reproducibly dysregulated genes in the study of myopia development[21 31 32 37 38] and is thought to exert an effect through modulating the extracellular matrix (ECM) of the sclera, in which SLC39A5 is abundantly expressed. Although the BMP/TGF-β pathway has been implicated in high myopia pathogenesis, the mechanism is still unclear. Our data suggest that zinc may be involved in eye development by regulating BMP/TGF-β, and disruption of this may cause the refractive error and finally result in the high myopia phenotype.

It is also worth highlighting that *SLC39A13* mutations caused under-hydroxylated lysyl and prolyl residues of collagens in EDS patients.[29] Since Slc39a13-deficient mouse presented with disruption of the BMP/TGF-β pathway,[30] there might be some kind of relationship between collagen or collagen hydroxylase and the BMP/TGF-β pathway. Indeed, BMP/TGF-β has been implicated in modulating ECM of the sclera,[39] which is mainly comprised of collagens. Therefore, it is possible that BMP/TGF-β may regulate the transcription of collagens or

collagen-related protein, such as lysyl and prolyl hydroxylase, and control the expression and normal function of collagens. The failure of any process may contribute to myopia or related phenotypes. Interestingly, one homozygous missense mutation in the prolyl hydroxylase encoded gene, *LEPREL1*, has been identified as the cause of autosome recessive high myopia in an Israeli family.[20] Furthermore, we also identified a homozygous loss-of-function mutation of this gene in a high myopia family from a Chinese population.[40] Further studies should be conducted to explore the relationship between collagen or collagen hydroxylase and the BMP/TGF-β pathway, as well as the potential underlying mechanism in the development of myopia.

Author affiliations
[1]The State Key Laboratory of Medical Genetics, Central South University, Changsha, Hunan, China
[2]School of Life Sciences, Central South University, Changsha, Hunan, China
[3]Department of Ophthalmology, The First Affiliated Hospital of Zhengzhou University, Zhengzhou, Henan, China
[4]Department of Ophthalmology, The Second Xiangya Hospital, Central South University, Changsha, Hunan, China
[5]Department of Dermatology, Institute of Dermatology, No. 1 Hospital, Anhui Medical University, Hefei, Anhui, China
[6]The Xiangya Hospital, Central South University, Changsha, Hunan, China
[7]Key Laboratory of Medical Information Research, Changsha, Hunan, China

Acknowledgements We greatly thank all the patients and their family members who participated in this study.

Contributors Conceived and designed the experiments: KX, ZH and HG. Performed the experiments: TZ, TW, HG, YP, AW, JC, YL, QT, LX, LZ, YP, LL and QL. Analysed the data: HG, TW and LS. Contributed reagents/materials/analysis tools: XJ, XZ, LS, LT, PT, YL and WX. Wrote the paper: HG and KX. Critically reviewed the manuscript: ZH, JL, WX, BT, YF, ZZ and QP. Obtained the funding: KX and ZH.

Funding The research was supported by the National Basic Research Program of China (2012CB517902), and the National Natural Science Foundation of China (81330027, 81161120544).

Competing interests None.

Patient consent Obtained.

Ethics approval The study was approved by the Institutional Review Board of The State Key Laboratory of Medical Genetics and adhered to the tenets of the Declaration of Helsinki.

Provenance and peer review Not commissioned; externally peer reviewed.

REFERENCES

1 He M, Zheng Y, Xiang F. Prevalence of myopia in urban and rural children in mainland China. *Optom Vis Sci* 2009;86:40–4.
2 Sawada A, Tomidokoro A, Araie M, Iwase A, Yamamoto T; Tajimi Study G. Refractive errors in an elderly Japanese population: the Tajimi study. *Ophthalmology* 2008;115:363–70.
3 Woo WW, Lim KA, Yang H, Lim XY, Liew F, Lee YS, Saw SM. Refractive errors in medical students in Singapore. *Singapore Med J* 2004;45:470–4.
4 Wong TY, Foster PJ, Hee J, Ng TP, Tielsch JM, Chew SJ, Johnson GJ, Seah SK. Prevalence and risk factors for refractive errors in adult Chinese in Singapore. *Invest Ophthalmol Vis Sci* 2000;41:2486–94.
5 Lyhne N, Sjolie AK, Kyvik KO, Green A. The importance of genes and environment for ocular refraction and its determiners: a population based study among 20–45 year old twins. *Br J Ophthalmol* 2001;85:1470–6.
6 Morgan IG, Ohno-Matsui K, Saw SM. Myopia. *Lancet* 2012;379:1739–48.
7 Hammond CJ, Snieder H, Gilbert CE, Spector TD. Genes and environment in refractive error: the twin eye study. *Invest Ophthalmol Vis Sci* 2001;42:1232–6.
8 Klein AP, Suktitipat B, Duggal P, Lee KE, Klein R, Bailey-Wilson JE, Klein BE. Heritability analysis of spherical equivalent, axial length, corneal curvature, and anterior chamber depth in the Beaver Dam Eye Study. *Arch Ophthalmol* 2009;127:649–55.
9 Hysi PG, Young TL, Mackey DA, Andrew T, Fernandez-Medarde A, Solouki AM, Hewitt AW, Macgregor S, Vingerling JR, Li YJ, Ikram MK, Fai LY, Sham PC, Manyes L, Porteros A, Lopes MC, Carbonaro F, Fahy SJ, Martin NG, van Duijn CM, Spector TD, Rahi JS, Santos E, Klaver CC, Hammond CJ. A genome-wide association study for myopia and refractive error identifies a susceptibility locus at 15q25. *Nat Genet* 2010;42:902–5.
10 Kiefer AK, Tung JY, Do CB, Hinds DA, Mountain JL, Francke U, Eriksson N. Genome-wide analysis points to roles for extracellular matrix remodeling, the visual cycle, and neuronal development in myopia. *PLoS Genet* 2013;9:e1003299.
11 Solouki AM, Verhoeven VJ, van Duijn CM, Verkerk AJ, Ikram MK, Hysi PG, Despriet DD, van Koolwijk LM, Ho L, Ramdas WD, Czudowska M, Kuijpers RW, Amin N, Struchalin M, Aulchenko YS, van Rij G, Riemslag FC, Young TL, Mackey DA, Spector TD, Gorgels TG, Willemse-Assink JJ, Isaacs A, Kramer R, Swagemakers SM, Bergen AA, van Oosterhout AA, Oostra BA, Rivadeneira F, Uitterlinden AG, Hofman A, de Jong PT, Hammond CJ, Vingerling JR, Klaver CC. A genome-wide association study identifies a susceptibility locus for refractive errors and myopia at 15q14. *Nat Genet* 2010;42:897–901.
12 Verhoeven VJ, Hysi PG, Wojciechowski R, Fan Q, Guggenheim JA, Hohn R, MacGregor S, Hewitt AW, Nag A, Cheng CY, Yonova-Doing E, Zhou X, Ikram MK, Buitendijk GH, McMahon G, Kemp JP, Pourcain BS, Simpson CL, Makela KM, Lehtimaki T, Kahonen M, Paterson AD, Hosseini SM, Wong HS, Xu L, Jonas JB, Parssinen O, Wedenoja J, Yip SP, Ho DW, Pang CP, Chen LJ, Burdon KP, Craig JE, Klein BE, Klein R, Haller T, Metspalu A, Khor CC, Tai ES, Aung T, Vithana E, Tay WT, Barathi VA, Consortium for Refractive EMyopiaChen P, Li R, Liao J, Zheng Y, Ong RT, Doring A, Diabetes Control and Complications Trial/Epidemiology of Diabetes Interventions and Complications Research GroupEvans DM, Timpson NJ, Verkerk AJ, Meitinger T, Raitakari O, Hawthorne F, Spector TD, Karssen LC, Pirastu M, Murgia F, Ang W, Wellcome Trust Case Control Consortium 2Mishra A, Montgomery GW, Pennell CE, Cumberland PM, Cotlarciuc I, Mitchell P, Wang JJ, Schache M, Janmahasatian S, Igo RP Jr, Lass JH, Chew E, Iyengar SK, Fuchs' Genetics Multi-Center Study GroupGorgels TG, Rudan I, Hayward C, Wright AF, Polasek O, Vatavuk Z, Wilson JF, Fleck B, Zeller T, Mirshahi A, Muller C, Uitterlinden AG, Rivadeneira F, Vingerling JR, Hofman A, Oostra BA, Amin N, Bergen AA, Teo YY, Rahi JS, Vitart V, Williams C, Baird PN, Wong TY, Oexle K, Pfeiffer N, Mackey DA, Young TL, van Duijn CM, Saw SM, Bailey-Wilson JE, Stambolian D, Klaver CC, Hammond CJ. Genome-wide meta-analyses of multiancestry cohorts identify multiple new susceptibility loci for refractive error and myopia. *Nat Genet* 2013;45:314–18.
13 Fan Q, Barathi VA, Cheng CY, Zhou X, Meguro A, Nakata I, Khor CC, Goh LK, Li YJ, Lim W, Ho CE, Hawthorne F, Zheng Y, Chua D, Inoko H, Yamashiro K, Ohno-Matsui K, Matsuo K, Matsuda F, Vithana E, Seielstad M, Mizuki N, Beuerman RW, Tai ES, Yoshimura N, Aung T, Young TL, Wong TY, Teo YY, Saw SM. Genetic variants on chromosome 1q41 influence ocular axial length and high myopia. *PLoS Genet* 2012;8:e1002753.
14 Khor CC, Miyake M, Chen LJ, Shi Y, Barathi VA, Qiao F, Nakata I, Yamashiro K, Zhou X, Tam PO, Cheng CY, Tai ES, Vithana EN, Aung T, Teo YY, Wong TY, Moriyama M, Ohno-Matsui K, Mochizuki M, Matsuda F, Nagahama Study GYong RY, Yap EP, Yang Z, Pang CP, Saw SM, Yoshimura N. Genome-wide association study identifies ZFHX1B as a susceptibility locus for severe myopia. *Hum Mol Genet* 2013;22:5288–94.
15 Li YJ, Goh L, Khor CC, Fan Q, Yu M, Han S, Sim X, Ong RT, Wong TY, Vithana EN, Yap E, Nakanishi H, Matsuda F, Ohno-Matsui K, Yoshimura N, Seielstad M, Tai ES, Young TL, Saw SM. Genome-wide association studies reveal genetic variants in CTNND2 for high myopia in Singapore Chinese. *Ophthalmology* 2011;118:368–75.
16 Shi Y, Gong B, Chen L, Zuo X, Liu X, Tam PO, Zhou X, Zhao P, Lu F, Qu J, Sun L, Zhao F, Chen H, Zhang Y, Zhang D, Lin Y, Lin H, Ma S, Cheng J, Yang J, Huang L, Zhang M, Zhang X, Pang CP, Yang Z. A genome-wide meta-analysis identifies two novel loci associated with high myopia in the Han Chinese population. *Hum Mol Genet* 2013;22:2325–33.
17 Shi Y, Qu J, Zhang D, Zhao P, Zhang Q, Tam PO, Sun L, Zuo X, Zhou X, Xiao X, Hu J, Li Y, Cai L, Liu X, Lu F, Liao S, Chen B, He F, Gong B, Lin H, Ma S, Cheng J, Zhang J, Chen Y, Zhao F, Yang X, Chen Y, Yang C, Lam DS, Li X, Shi F, Wu Z, Lin Y, Yang J, Li S, Ren Y, Xue A, Fan Y, Li D, Pang CP, Zhang X, Yang Z. Genetic variants at 13q12.12 are associated with high myopia in the Han Chinese population. *Am J Hum Genet* 2011;88:805–13.
18 Shi Y, Li Y, Zhang D, Zhang H, Li Y, Lu F, Liu X, He F, Gong B, Cai L, Li R, Liao S, Ma S, Lin H, Cheng J, Zheng H, Shan Y, Chen B, Hu J, Jin X, Zhao P, Chen Y, Zhang Y, Lin Y, Li X, Fan Y, Yang H, Wang J, Yang Z. Exome sequencing identifies ZNF644 mutations in high myopia. *PLoS Genet* 2011;7:e1002084.
19 Tran-Viet KN, Powell C, Barathi VA, Klemm T, Maurer-Stroh S, Limviphuvadh V, Soler V, Ho C, Yanovitch T, Schneider G, Li YJ, Nading E, Metlapally R, Saw SM, Goh L, Rozen S, Young TL. Mutations in SCO2 are associated with autosomal-dominant high-grade myopia. *Am J Hum Genet* 2013;92:820–6.
20 Mordechai S, Gradstein L, Pasanen A, Ofir R, El Amour K, Levy J, Belfair N, Lifshitz T, Joshua S, Narkis G, Elbedour K, Myllyharju J, Birk OS. High myopia caused by a mutation in LEPREL1, encoding prolyl 3-hydroxylase 2. *Am J Hum Genet* 2011;89:438–45.

21 Aldahmesh MA, Khan AO, Alkuraya H, Adly N, Anazi S, Al-Saleh AA, Mohamed JY, Hijazi H, Prabakaran S, Tacke M, Al-Khrashi A, Hashem M, Reinheckel T, Assiri A, Alkuraya FS. Mutations in LRPAP1 are associated with severe myopia in humans. *Am J Hum Genet* 2013;93:313–20.
22 Abecasis GR, Cherny SS, Cookson WO, Cardon LR. Merlin—rapid analysis of dense genetic maps using sparse gene flow trees. *Nat Genet* 2002;30:97–101.
23 Li H, Durbin R. Fast and accurate short read alignment with Burrows-Wheeler transform. *Bioinformatics* 2009;25:1754–60.
24 McKenna A, Hanna M, Banks E, Sivachenko A, Cibulskis K, Kernytsky A, Garimella K, Altshuler D, Gabriel S, Daly M, DePristo MA. The Genome Analysis Toolkit: a MapReduce framework for analyzing next-generation DNA sequencing data. *Genome Res* 2010;20:1297–303.
25 Li H, Handsaker B, Wysoker A, Fennell T, Ruan J, Homer N, Marth G, Abecasis G, Durbin R; Genome Project Data Processing S. The sequence alignment/Map format and SAMtools. *Bioinformatics* 2009;25:2078–9.
26 Wang K, Li M, Hakonarson H. ANNOVAR: functional annotation of genetic variants from high-throughput sequencing data. *Nucleic Acids Res* 2010;38:e164.
27 Wang F, Kim BE, Petris MJ, Eide DJ. The mammalian Zip5 protein is a zinc transporter that localizes to the basolateral surface of polarized cells. *J Biol Chem* 2004;279:51433–41.
28 Pocanschi CL, Ehsani S, Mehrabian M, Wille H, Reginold W, Trimble WS, Wang H, Yee A, Arrowsmith CH, Bozóky Z, Kay LE, Forman-Kay JD, Rini JM, Schmitt-Ulms G. The ZIP5 ectodomain co-localizes with PrP and may acquire a PrP-like fold that assembles into a dimer. *PLoS ONE* 2013;8:e72446.
29 Giunta C, Elcioglu NH, Albrecht B, Eich G, Chambaz C, Janecke AR, Yeowell H, Weis M, Eyre DR, Kraenzlin M, Steinmann B. Spondylocheiro dysplastic form of the Ehlers-Danlos syndrome—an autosomal-recessive entity caused by mutations in the zinc transporter gene SLC39A13. *Am J Hum Genet* 2008;82:1290–305.
30 Fukada T, Civic N, Furuichi T, Shimoda S, Mishima K, Higashiyama H, Idaira Y, Asada Y, Kitamura H, Yamasaki S, Hojyo S, Nakayama M, Ohara O, Koseki H, Dos Santos HG, Bonafe L, Ha-Vinh R, Zankl A, Unger S, Kraenzlin ME, Beckmann JS, Saito I, Rivolta C, Ikegawa S, Superti-Furga A, Hirano T. The zinc transporter SLC39A13/ZIP13 is required for connective tissue development; its involvement in BMP/TGF-beta signaling pathways. *PLoS ONE* 2008;3:e3642.
31 Jobling AI, Wan R, Gentle A, Bui BV, McBrien NA. Retinal and choroidal TGF-beta in the tree shrew model of myopia: isoform expression, activation and effects on function. *Exp Eye Res* 2009;88:458–66.
32 Seko Y, Shimokawa H, Tokoro T. Expression of bFGF and TGF-beta 2 in experimental myopia in chicks. *Invest Ophthalmol Vis Sci* 1995;36:1183–7.
33 Matsumoto M, Funami K, Tanabe M, Oshiumi H, Shingai M, Seto Y, Yamamoto A, Seya T. Subcellular localization of Toll-like receptor 3 in human dendritic cells. *J Immunol* 2003;171:3154–62.
34 Langer G, Bader B, Meoli L, Isensee J, Delbeck M, Noppinger PR, Otto C. A critical review of fundamental controversies in the field of GPR30 research. *Steroids* 2010;75:603–10.
35 Huibi X, Kaixun H, Qiuhua G, Yushan Z, Xiuxian H. Prevention of axial elongation in myopia by the trace element zinc. *Biol Trace Elem Res* 2001; 79:39–47.
36 Shiue C, Ko LS. Study on serum copper and zinc levels in high myopia. *Acta Ophthalmol Suppl* 1988;185:141–2.
37 Chen BY, Wang CY, Chen WY, Ma JX. Altered TGF-beta2 and bFGF expression in scleral desmocytes from an experimentally-induced myopia guinea pig model. *Graefes Arch Clin Exp Ophthalmol* 2013;251:1133–44.
38 Lam DS, Lee WS, Leung YF, Tam PO, Fan DS, Fan BJ, Pang CP. TGFbeta-induced factor: a candidate gene for high myopia. *Invest Ophthalmol Vis Sci* 2003;44:1012–15.
39 Jobling AI, Nguyen M, Gentle A, McBrien NA. Isoform-specific changes in scleral transforming growth factor-beta expression and the regulation of collagen synthesis during myopia progression. *J Biol Chem* 2004;279:18121–6.
40 Guo H, Tong P, Peng Y, Wang T, Liu Y, Chen J, Li Y, Tian Q, Hu Y, Zheng Y, Xiao L, Xiong W, Pan Q, Hu Z, Xia K. Homozygous loss-of-function mutation of the LEPREL1 gene causes severe non-syndromic high myopia with early-onset cataract. *Clin Genet* 2013 Oct 30. doi: 10.1111/cge.12309.